Femtosecond pump probe spectroscopy for the study of energy transfer of light-harvesting complexes from extractions of spinach leaves

S. Ombinda-Lemboumba[a,b], A. du Plessis[a,b*], R.W. Sparrow[c], P. Molukanele[a,c], L.R. Botha[a,b], E.G. Rohwer[b], C.M. Steenkamp[b] and L. van Rensburg[d]

Measurements of ultrafast transient processes, of temporal durations in the picosecond and femtosecond regime, are made possible by femtosecond pump probe transient absorption spectroscopy. Such an ultrafast pump probe transient absorption setup has been implemented at the CSIR National Laser Centre and has been applied to investigate energy transfer processes in different parts of photosynthetic systems. In this paper we report on our first results obtained with Malachite green as a benchmark. Malachite green was chosen because the lifetime of its excited state is well known. We also present experimental results of the ultrafast energy transfer of light-harvesting complexes in samples prepared from spinach leaves. Various pump wavelengths in the range 600–680 nm were used; the probe was a white light continuum spanning 420–700 nm. The experimental setup is described in detail in this paper. Results obtained with these samples are consistent with those expected and achieved by other researchers in this field.

Key words: pump probe spectroscopy, ultrafast spectroscopy, transient absorption, femtosecond laser, light-harvesting complex II, Malachite green

Introduction

Photosynthesis is the process by which light energy is converted into chemical energy and then, through a complex series of biochemical and biophysical processes, to any one of a number of bio-machines.[1] There is a large diversity of photosynthetic organisms—higher plants, cyanobacteria and photosynthetic bacteria[2] —for which some fundamental processes are common. These are light absorption, excitation energy transfer, charge separation and vectoral charge transfer.[1] In the photosynthetic process, chlorophylls are light-absorbing pigments which bind to proteins and are also known as pigment proteins. These pigment proteins have two main functions. They form light-harvesting antenna complexes which are organised into an antenna system to absorb light and transfer the excitation energy to the second functional entity called a reaction centre. It is at the reaction centre that charge separation and transfer occurs.[1,3]

In the natural state there is a high degree of disorder within the system. This is due to natural light from the sun irradiating the photosynthetic pigments with a range of different wavelengths of light which the pigments can absorb. This means that the energy of the photons, the intensity of the light and the time between photon excitations occurs in a random manner. The environmental conditions in which these systems grow also vary.[4] In order to investigate the processes of light absorption and energy transfer, these variables need to be reduced, and a number of strategies are used. Over recent years, several photosynthetic components have been isolated and detailed structural information obtained using crystallographic data[5–7] and atomic force microscopy.[8–10] A significant amount of the work on elucidating the structures of energy transfer processes within light-harvesting complexes (LHCs) and reaction centres has been conducted on purple photosynthetic bacteria.[2] In photosynthetic organisms, such as the bacteria *Rhodobacter sphaeroides,* there are two types of light-harvesting antenna complexes—types 1 and 2. These are termed LH1 (B875) and LH2 (B800/850). In the more general case of non-bacterial organisms, these light-harvesting complexes are termed LHC I and LHC II. LHC II acts as a light-absorbing and transferring complex. LHC I is closely associated with a reaction centre.[11,12] In all species of purple bacteria, the LHC I surrounds the reaction centre.[2] However, LHC I and LHC II are constructed on the same modular basis.[13,14] This organisation of reaction centres surrounded by aggregates of chlorophylls and associated carotenoids, seems to be universal to photosynthetic bacteria and higher plants and is called the photosynthetic unit.[15] When photons are absorbed by one of the chromophores in the LHC II antenna complex, non-radiative photophysical processes occur in a series that channels the excitation energy with high efficiency from the site of absorption. There are two types of ultrafast photophysical processes that occur. One type is energy migration (exciton process), which is the reversible series of energy transfer processes that occurs between identical coupled chromophores – in this case between LHC II antenna complexes of the photosynthetic membrane. The other type is energy transfer, which refers to the down-hill energy transfer process which will then terminate the exciton process[16] within the photosynthetic unit. Energy transfer takes place in the order LHC II → LHC I → reaction centre. An irreversible electron transfer reaction occurs at a special pair of chromophores in the reaction centre, preventing any possible back transfer of energy.[16] Both of these occur in the singlet state of an excited pigment.[16] The energy transfer is a sequential process, is multi-exponential and occurs in a total time of less than 100 ps, at about 95% efficiency.[15] Within a bacteriochlorophyll ring, it is estimated that energy transfer around the ring takes place in a few hundred femtoseconds.[17,18] The LH2 → LH1 transfer time is 3–5 ps[19] and energy transfer from LH1 → reaction centre is 30–50 ps.[20] This longer time is due to the greater LH1–reaction-centre distance. Energy migration times are strongly dependent on the relative orientation of the transition moments within the macrocycle array.

One line of study is to isolate these functional components and study the energy transfer characteristics separately. The energy transfer processes of these photosynthetic systems can be investigated using ultrafast pump probe transient absorption spectroscopic techniques.[21–23] The use of ultrafast pulsed lasers enables the pigments to be excited in unison with a quasi-mono-

[a]CSIR National Laser Centre, P.O. Box 395, Pretoria 0001, South Africa.
[b]Laser Research Institute, Department of Physics, University of Stellenbosch, Private Bag X1, Matieland 7602, South Africa.
[c]CSIR Biosciences, P.O. Box 395, Pretoria 0001, South Africa.
[d]Environmental Science and Management, North-West University, Private Bag X6001, Potchefstroom 2520, South Africa.
*Author for correspondence E-mail: adplessis2@csir.co.za

chromatic light source. This pump pulse excites the pigments at a pre-set temporal origin, after which the energy transfer can be probed by a second pulse with an adjustable delay.[4] In our experiment, the sample used was isolated LHC II from spinach leaves.

The LHC II is the most abundant antenna in the photosystem II. The function of the LHC II is to transfer excitation energy towards a reaction centre of either photosystem I (PS I) or photosystem II (PS II). Normally, there are four LHC II trimers per PS II reaction centre.[24] In addition to LHC II, the PS II contains other complexes such as CP29, CP26, CP47, CP43, D1 and D2. The CP43, CP47, D1 and D2 form the PS II core complex.[25–27] In its native form, the LHC II is a trimeric protein. The structure of this complex was first described in 1994 by Kühlbrant *et al.*[29] Each monomer contains 7–8 chlorophyll *a* molecules, 4–5 chlorophyll *b* molecules and 3 carotenoids, namely lutein, neoxanthin and violaxanthin.[28,29] These chlorophylls have been assigned specific site energies. The site energies of chlorophyll *a* are 602–604 and 610–614, those for chlorophyll *b* are 601 and 605–609.[5] These chlorophylls are arranged in two separate layers: one close to the stromal surface and the other by the luminal surface with a distance ranging from 13.9–18 Å between them. Close to the stromal surface of the membrane are three clusters of chlorophylls. There is a chlorophyll *a* trimer (a610–a611–a612) and a chlorophyll *a* dimer (a602–a603). These are closely associated with three chlorophyll *b* molecules (b601, b608 and b609). On the luminal side of the membrane there is a chlorophyll *a* cluster (a613 and a614), a group of chlorophyll *b* (b606, b607 and b605) and a single chlorophyll *a* (a604).[30] When assembled, the LHC II trimer contains between 36 and 42 chlorophyll molecules as well as 10 to 12 xanthophyll (lutein, neoxanthin and violaxanthin) molecules. *In vivo* and *in vitro,* there is a further level of structural organisation that LHC II can adopt. This is either a regular lamellar sheet, usually 2D in shape, or, alternatively, in a 3D or disordered 3D structure.[31] Thus, LHC II has a large degree of flexibility in its structural organisation, with accompanying changes in optical properties.

The interpretation of pump probe transient absorption data is highly complex and the results obtained are influenced by many factors, such as the degree of aggregation of the LHC II[25] or whether the complexes are in the monomeric or trimeric state.[25,32] However, in this study, the main focus of the research is not on elucidating the photophysical processes of photosynthetic energy transfer. We propose to develop light-harvesting and energy-transfer systems with architectures to enable specific, site-directed energy transfer. Our aim is to characterise these systems with respect to the direction, efficiency and rate of energy transfer from the site of photon absorption to the terminal energy transfer process. We report these preliminary results as a proof of principle of our experimental setup, using Malachite green dye, and to indicate the presence of the above-mentioned energy transfer processes in LHC II extractions from spinach leaves.

Background

Many biological and chemical processes occur on relatively long time scales (from milliseconds to seconds). These long processes are the result of combinations of several very fast elementary processes ranging from femtoseconds to picoseconds.[33] This generally is referred to as the ultrafast or ultrashort pulse regime. In order to observe ultrafast processes, such as the translation or rotation of part of a molecule, energy transfer, charge transport or the formation or breaking of a chemical bond, a measurement technique with a temporal resolution in the range of femtoseconds to picoseconds is required. However, most detectors are not fast enough to resolve such time scales.

Femtosecond transient absorption (pump probe) spectroscopy has become a widely-used and useful technique for studying ultrafast processes.[34]

In the pump probe spectroscopy technique, a beam consisting of a train of ultrafast laser pulses is split into pump and probe beams. The pump and probe beams are sent along different optical paths, and then focused into a sample with a time delay between them.[35] The pump is used to trigger a photoinduced process in the sample and the probe beam is used to probe the process, for example molecules or atoms in their excited states. The evolution of this process is then followed by monitoring the delayed probe pulse, for example by absorption, and varying this delay time. The resulting spectra are therefore measured at a range of delay times to provide transient absorption at a range of wavelengths.

The pump-induced variation of the probe absorbance (ΔA) as a function of delay time can be measured and analysed. This is done by observing pumped as well as non-pumped probe spectra. Using the Beer-Lambert law for linear absorption in a liquid sample, the ΔA can be written as:

$$\Delta A = A_{\text{pumpON}} - A_{\text{pumpOFF}} = \log\left(\frac{I_{\text{I}}}{I_{\text{signal}}}\right)_{\text{ON}} - \log\left(\frac{I_{\text{I}}}{I_{\text{signal}}}\right)_{\text{OFF}}, \quad (1)$$

where I_{I} is the incident intensity and I_{signal} the transmitted intensity. Considering that I_{ref} is proportional to I_{I} in the setup depicted in Fig. 1, the absorbance change is given by:

$$\Delta A = A_{\text{pumpON}} - A_{\text{pumpOFF}} = \log\left(\frac{I_{\text{ref}}}{I_{\text{signal}}}\right)_{\text{ON}} - \log\left(\frac{I_{\text{ref}}}{I_{\text{signal}}}\right)_{\text{OFF}}. \quad (2)$$

This equation indicates that the absorbance change (ΔA) is a function of the ratio of the reference and probe signals at a given wavelength, measured after the sample excitation ('on'), and of the ratio of the same signals measured in an unexcited sample ('off').

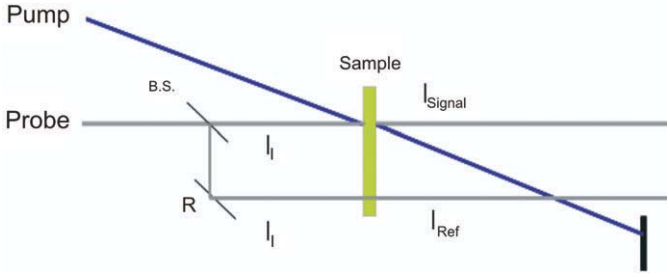

Fig. 1. The overlap of pump and probe beams. The two probe beams are shown: the signal and the reference.

In order to benchmark our experimental setup, Malachite green dye was used as a sample. Several spectroscopic studies have been conducted on Malachite green. Previously measured ultrafast pump probe signals have shown that Malachite green has an ultrashort electronic excited state lifetime that depends on the solvent viscosity but is in the region of 3 ps.[36] In another study, transient absorption signals of Malachite green in ethanol solution, pumped at 580 nm and probed at 620 nm, showed a fast kinetic process with a time constant of approximately 2.1 ps.[37]

There has been considerable research directed towards developing artificial photosynthetic systems and a number of groups have synthesised artificial light-harvesting, energy migration and charge transfer components.[38–41] In this collaborative research effort between the Femtosecond Science Group and the Synthetic Biology Group of the Council for Scientific and Industrial Research (CSIR), the aim was to use ultrafast pump probe

spectroscopy to determine energy transfer times experimentally for both natural and artificial light-harvesting systems. It is envisaged that we will explore a range of pigments from higher plants as well as photosynthetic bacteria arrayed in a variety of organisational configurations. One of the goals is to establish the distance over which energy can be transferred. It is also envisaged that polymeric structures will be used as an architectural scaffold onto which the pigments will be attached. With this arrangement it should be possible to develop multi-pigment systems for directed energy transfer.

Sample preparation and characterisation: LHC II

Isolation and characterisation of loosely stacked lamellar aggregates of LHC II with long-range chiral order

LHC II samples were prepared from spinach leaves (with good turgor and dark green colour) as described before[42] with a few modifications to suit the experimental conditions. The leaves were grown at a local greenhouse and the entire experiment was performed under normal laboratory light and on ice. spinach leaves were washed with cold water and chilled distilled water, and then homogenised in a blender with ice-cold buffer A (50 mM Hepes, 0.4 M sorbitol, pH 7.8 with NaOH). The suspension was filtered through four layers of muslin and then centrifuged at 5 000 *g* for 5 min at 4°C. The pellet was resuspended in cold buffer B (20 mM Hepes, 5 mM EDTA, 50 mM sorbitol, pH 7.8 with NaOH). A medium-sized brush was used for crude homogenisation of the pellet to ensure all material was finely homogenised without large visible particles. The suspension was again centrifuged at 10 000 *g* for 10 min at 4°C. The pellet was resuspended in cold buffer C (20 mM Hepes, pH 7.8 with NaOH) and again homogenised as above. Triton x-100 was added to the suspension to obtain the final detergent concentration of 0.7–0.9%, and the suspension was then stirred continuously on ice and in the dark for at least 45 min, followed by centrifugation at 30 000 *g* for 40 min at 4°C. The supernatant predominantly contained LHC II and hence was kept at this stage and the pellet was discarded. All the centrifugation procedures were carried out using a Beckman Coulter, Avanti J-30I centrifuge. The preparations can be stored in the dark at –87°C for up to a month without the loss of their lamellar structure. Thawing and refreezing can lead to complete destruction of these properties, therefore a sample can be used only once. The prepared sample was diluted in Buffer C to obtain an absorbance of ~1 in a 1-cm optical pathlength cuvette at 430 nm for all the characterisation methods as well as the pump probe experiments. The chlorophyll content of the sample was calculated using a method based on Arnon's equations: Add 50 μl sample, 10 cm^3 of 80% v:v acetone, filter and read absorbance at 665 nm and 649 nm. Arnon's equations are given by:

$$\text{Chlorophyll } a = [(A_{665} \times 11.63) - (A_{649} \times 2.39)] \times 0.2 \text{ mg cm}^{-3}$$

$$\text{Total chlorophyll} = [(A_{665} \times 6.4) + (A_{649} \times 17.72)] \times 0.2 \text{ mg cm}^{-3}$$

$$\text{Chlorophyll } b = \text{Total chlorophyll} - \text{chlorophyll } a,$$

where A_{665} and A_{649} are the absorbance of the sample at 665 nm and 649 nm. By using these equations we found the following values: Chlorophyll a = 1.68 mg cm^{-3}, chlorophyll b = 0.69 mg cm^{-3}, total chlorophyll content = 2.38 mg cm^{-3} and chlorophyll a/b ratio = 2.4:1

Characterisation methods

Circular dichroism measurements

Circular dichroism (CD) was measured at room temperature using the Chirascan Circular Dichroism Spectrometer (Applied Photophysics) and the results can be presented in units of absorbance or millidegrees (mdeg). LHC II, when isolated with mild detergent treatments, readily assembles into loosely stacked lamellar aggregates, which exhibits a significant degree of long-range chiral order of their chromophores. Long-range chirality is in turn essential for long distance energy migration. This characteristic of LHC II is essential for the purposes of this study: to prepare a LHC II sample that can undergo energy migration. This is evident when the CD spectrum of LHC II is observed in Fig. 2. The asymmetric bands (psi-type CD band) at ~430–505 nm and ~675 nm indicate the formation of large macro-aggregates with long-range chiral order within the sample, which allows energy transfer.

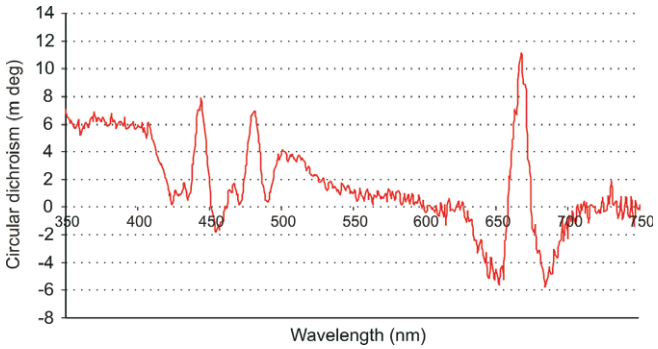

Fig. 2. Circular dichroism spectrum of loosely-stacked lamellar aggregates of LHC II (Type II).

Sodium dodecyl sulphate polyacrylamide gel electrophoresis (SDS-PAGE)

A SDS-PAGE gel of 12% acrylamide was cast (using a Bio-Rad mini-protean tetra cell and PowerPac universal). This technique was performed to identify proteins in the sample mixture. Figure 3 illustrates the results obtained from performing the SDS-PAGE using the extracted LHC II sample at room temperature. Lane 1 contained protein molecular makers, while Lanes 2 to 7 contained LHC II sample buffered with a 5× sample buffer in different concentrations to obtain optimal resolution. Lanes 2 to 4 contained a sample that was more concentrated and gave a better resolution, while Lanes 5 to 7 contained sample that was strongly diluted (with little protein) and hence very difficult to see using Coomassie blue staining solution. Results obtained from this technique showed that the prepared sample contained mostly LHC II complexes and this can be seen from the broken-down complexes of PS II, as shown in Fig. 3. CP47 (45k–50kDa) and CP43 (35 kDa), which are complexes from the peripheral core complex of PS II, together with D1 and D2 proteins closely associated to the reaction centre, were present; pure LHC II (56 kDa) was also present. All these pigment protein complexes could be detected using Coomassie blue staining solution. The gel also indicated the presence of small subunits (20–25 kDa) from LHC I and CPI. This implies that the sample was not purely LHC II; it contained some components from LHC I as well as some from PS II reaction centre.

Experimental setup

A generic femtosecond pump probe experimental setup was used and is described below. A commercial Ti:sapphire femtosecond oscillator (Coherent Mira 900-F), operating at a repetition rate of 76 MHz and pumped by the 5 W output of a continuous diode-pumped Nd:YVO_4 laser (Coherent Verdi V5), produced pulses of approximately 130 fs duration, as measured by a home-built autocorrelator. These pulses were stretched and then amplified by a regenerative Ti:sapphire amplifier (Coherent Legend-F) pumped by a diode-pumped, Q-switched

Nd:YLF laser (Coherent Evolution) at a repetition rate of 1 kHz, and finally compressed to produce 130-fs pulses of up to 1 mJ per pulse. This pulse duration was also measured by a home-built autocorrelator. These pulses have a bandwidth of about 8-nm full-width-at-half-maximum (FWHM) and a central wavelength of 795 nm.

As shown in Fig. 4, the amplified beam is split by a beam splitter (BS1) into two beams (90% transmitted and 10% reflected)—the pump and probe beams, respectively. The probe beam is sent to a variable optical delay line, which comprises a retro-reflector mirror on a precision translation stage controlled by a computer. The probe beam is then focused on a 2.15-mm-thick sapphire plate to generate a white light continuum. A short pass filter is placed after the plate in the probe path in order to suppress the strong residual peak, at 795 nm, from the Ti:sapphire laser. The probe beam is split into two beams—reference and signal. The signal is focused on the sample in such a way that it overlaps spatially with the pump beam in the liquid sample, while the reference beam is also sent through the sample, as indicated in Fig. 1. The pump pulse is sent through an optical parametric amplifier (TOPAS C – OPA) in order to obtain a wide tuning range of the pump beam (530–20000 nm). After the optical parametric amplifier, a chopper is inserted in the pump beam path in order to record spectra that are classified as pumped and not-pumped, thereby reducing background effects. The probe reference and signal beams are focused on optical fibres which guide the beams into the entrance slit of an imaging spectrometer. The spectrometer (MS 2004 I) uses a Czerny-Turner optical configuration. The light, after passing through the entrance slit, is directed by a collimating spherical mirror onto a diffraction grating. The grating used in this study is 600 lines per mm diffraction grating, blazed at 500-nm for 330-nm to 1 000-nm operation. The grating disperses the entrance parallel beams (signal and reference beams), and these are again collimated, using a second collimating mirror, onto two vertically-separated photodiode arrays. This spectrometer disperses both beams to a maximum of 206 nm across the active area of the photodiode arrays. Each photodiode array has 1024 pixels and a spectral response range from 200 nm to 1000 nm. All pump probe measurements were performed at room temperature and in dark conditions. The sample was held in a rotating cuvette cell of 1-mm thickness. Unless otherwise specified, averaging was done over 100 pulses per measurement at each delay time. The entire pump probe setup described above is a commercial system from CDP systems, the ExciPro-D.

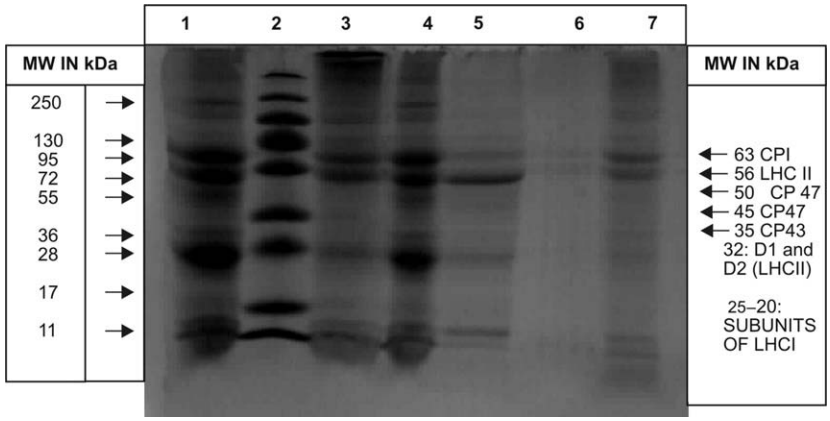

Fig. 3. SDS-PAGE image of extracted LHC II scanned using a Vacutec® G:Box from Syngene (Johannesburg, South Africa).

Experimental results and discussion

Malachite green

A white light continuum was generated using a sapphire plate in order to use this as a probe pulse in the pump probe experiment. Figure 5 shows spectra of the white light continuum,

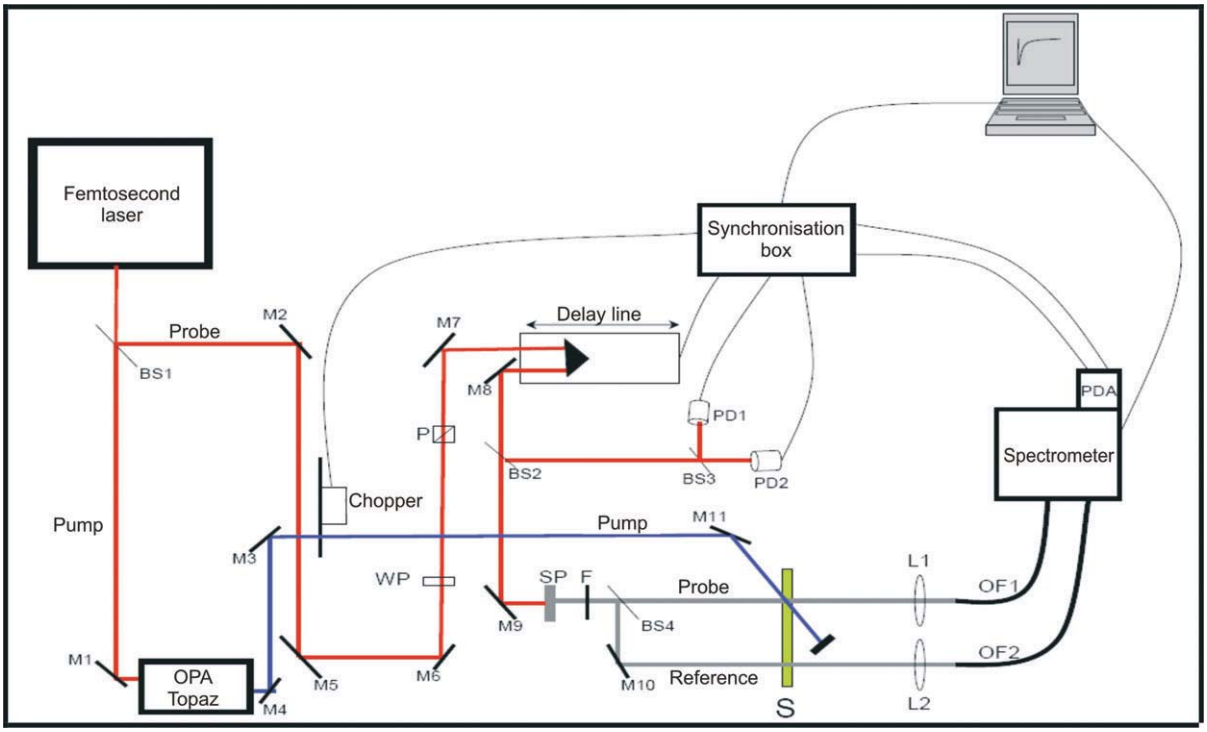

Fig. 4. Pump-probe experimental setup used to measure transient absorption in liquid samples. BS1–4: beam splitters; M1–11: coated mirrors; WP: wave plate; P: polariser; SP: sapphire plate; F: cut-off filter; S: sample; PD1 and PD2: photodiodes; L1 and L2: focusing lenses; OF1 and OF2: optical fibres; PDA: photodiode array; OPA: optical parametric amplifier.

recorded using an Ocean Optics USB 2000 spectrometer. Two spectra are shown, with and without a short-pass filter, in order to illustrate the strong residual signal from the 795-nm laser output and hence the need for the short-pass filter. This white light was then split, using a 50:50 beam splitter, into two: the probe and reference beams. Malachite green in ethanol was used as a sample for this proof of principle experiment, to demonstrate the working of the system. A typical result of the pump probe transient absorption signal, at one particular wavelength, is shown in Fig. 6. In this experiment, the pump pulse energy was 1.5 μJ with a focused beam size of about 300 μm. The 610-nm absorption change as a function of delay time is presented here. Since the optical parametric amplifier was set also to 610 nm (pump wavelength), this is effectively a one-colour pump probe measurement, although the probe is in fact a white light continuum and therefore more information is available from a single experiment. The temporal delay time at which the strongest absorption change (0.045 OD) is observed is relative to the physical position of the retro-reflector in the optical delay line, and has not been calibrated for zero position. We observe a fast decay process after this point, which can be attributed to the excited state decay as expected. A single exponential fit of the decay data, which seems to fit reasonably well in this case, indicates a time constant of 2.9 ± 0.1 ps.

Figure 7 shows a contour graph of the measured transient absorption of the Malachite green for the entire wavelength range 500–720 nm. It can be seen in this figure that the strongest absorption change occurs at about 620 nm and no other absorption changes of interest occur in this range, as expected.[36,37] The maximum absorbance changes for our experimental measurements were between 0.055 OD and 0.060 OD, and the noise level was 0.002 OD. The temporal resolution depends on the pulse duration of the pump pulse (130 fs), the degree of chirp of the white light continuum and the step size of the delay line. The temporal resolution was better than 200 fs in all experiments reported here, and was obtained experimentally by inference from the data recorded for Malachite green, as indicated in Fig. 8; this resolution is a compromise between error margins obtained and the total time required for the completion of a single experiment.

White light continuum chirp measurement and correction

The white light continuum is obtained by focusing a femtosecond pulse onto an

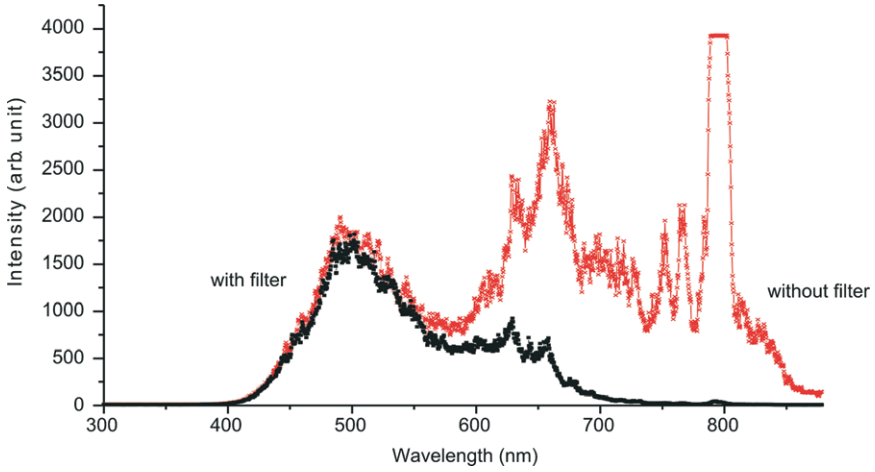

Fig. 5. Spectra of the white light continuum used in the non-linear crystal pump probe system, with and without a short-pass filter.

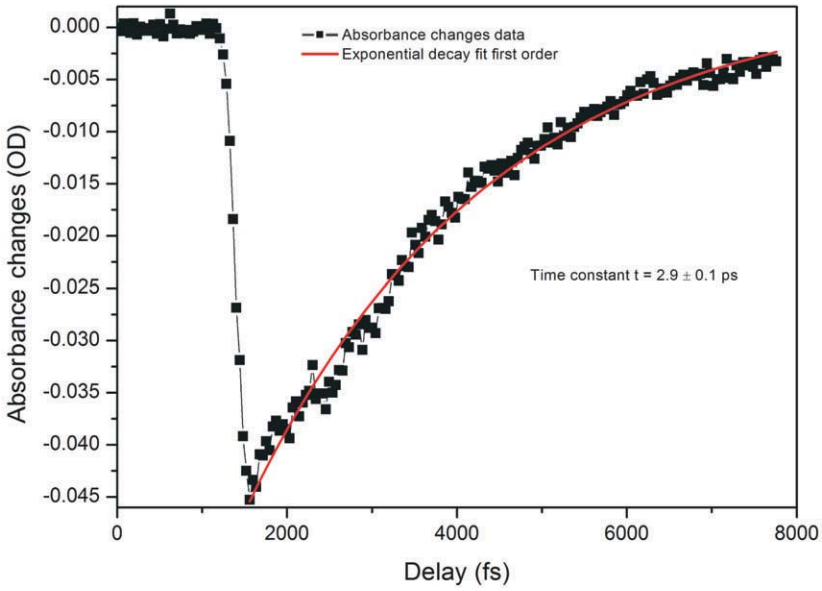

Fig. 6. Absorbance change at 610 nm as a function of delay between pump and probe pulses in malachite green. In this case the pump was set to 610 nm and the probe was a white light continuum.

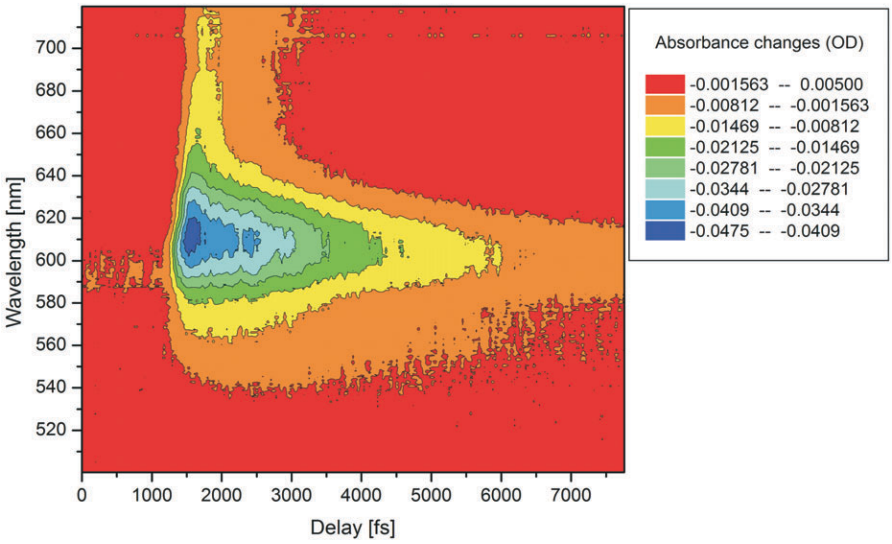

Fig. 7. Transient absorption contour graph indicating measured absorbance spectra for a range of delay times between pump and probe pulses. The strongest absorbance change occurred at 610 nm and at a relative delay of 1 900 fs in this experiment.

optical medium (a sapphire plate in our case). The propagation of the femtosecond pulse through this medium leads to spectral broadening (which is useful in this experiment), but also temporal lengthening of the pulse due to chirp. This chirp is due to the spectral components with low-frequency (red components) propagating faster than those with higher frequency (blue components). Therefore, different wavelength components in the probe pulse arrive at different times at the sample. It is important to correct for the chirp introduced by the white light generation in the analysis of the pump probe results.

The effect of this chirp is that the relative delay between the pump pulses and the different wavelength components of the white light spectrum will be different, and dependent on the amount of chirp induced. To correct this, one must compensate these delay differences, which requires that the kinetics of a known specimen, which exhibits a localised temporal response in the spectral range of interest, must be recorded. In our experiment, we used dyes as specimens with localised temporal response in the spectral range from 400 nm to 700 nm (Oxazine 170 and sulphorhodamine B dyes). Pump probe measurements were done on Oxazine 170 and sulphorhodamine B, and the absorbance change spectra and kinetics were recorded. These experiments were carried out with a pump energy measured at the laser output of 35.51 μJ, which resulted in roughly 1.2 μJ before the sample, by the appropriate use of filters. The goal was to plot relative time delay versus the wavelength of the dye. For every wavelength of the Oxazine 170 recorded spectra (Fig. 9, inner graph), a corresponding kinetics graph (Fig. 9, outer graph) was determined and a corresponding delay time, which corresponded best to the overlap between pump and that particular probe wavelength, was extracted. When a kinetics spectrum is obtained, 90% and 10% of the maximum value of the absorbance change is determined. In order to find the corresponding time delay of a specific wavelength, first a value of absorbance change at half of the difference between these two values (90% and 10% of maximum absorbance change) is found. Then a corresponding time is determined, as indicated in Fig. 9. A set of relative delay time values are then obtained for the 400–700-nm spectral range. It is therefore possible to plot the relative time delay against the wavelength. Figure 9 shows the plot of relative time delay against the wavelength of two different dyes: Oxazine 170 and sulphorhodamine B. As expected, it was observed that, under the same conditions, the two dyes exhibited the same behaviour (Fig. 10). In Fig. 10, it can be seen that, as the wavelength increases (from blue toward red) the relative time delay increases and the white light spectrum in our experiment, which ranges from 410 nm to 710 nm, has a total temporal span of about 1.6 ps. To obtain the chirp correction equation, data from the plot of relative time delay against wavelength, using Oxazine 170, was polynomial fitted. Figure 10 shows the third-order polynomial fit, as well as the polynomial equation (in red). This equation was used to correct for the chirp introduced by the white light in further analyses of other samples.

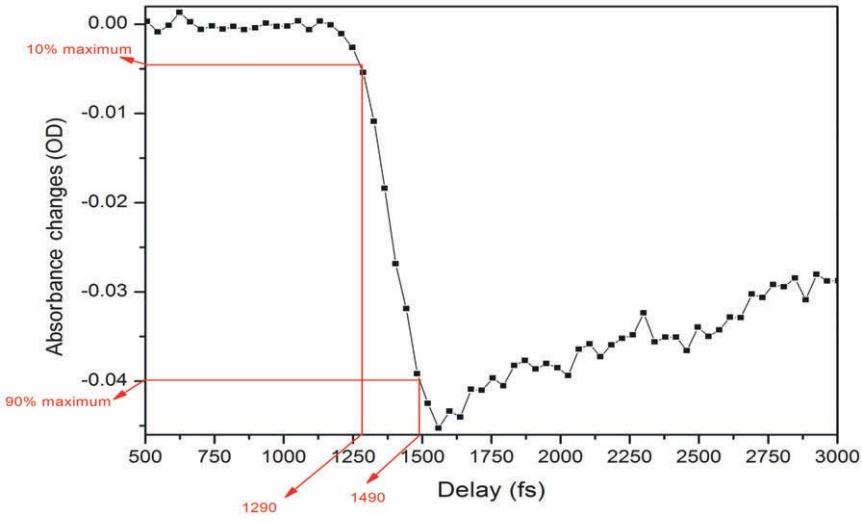

Fig. 8. Transient absorption kinetics of malachite green obtained by using a step size of 20 (1 step = 0.78 fs).

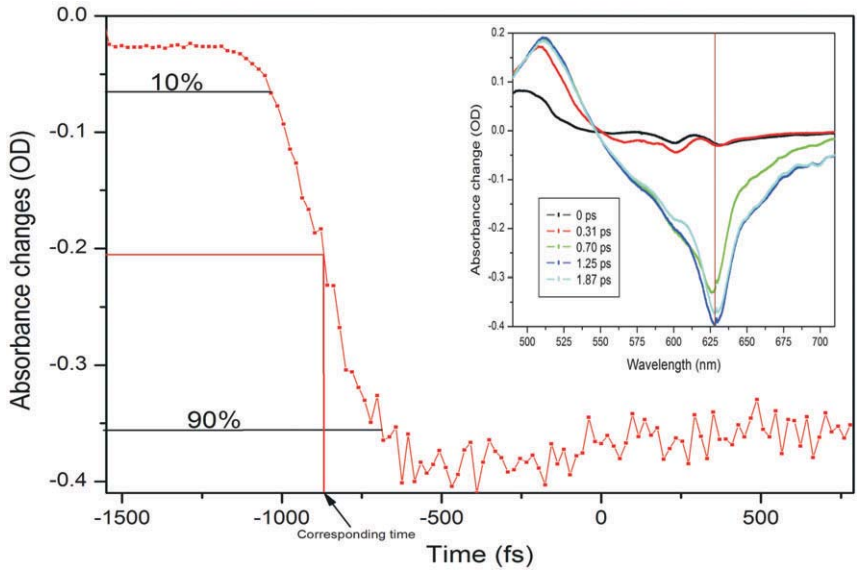

Fig. 9. Absorbance change at 628 nm as a function of delay between pump and probe pulses (outer graph) and transient absorption in the indicated wavelength interval and time delay (inner graph) of Oxazine 170 dye with pump wavelength set at 560 nm.

Light-harvesting complex II

The absorption spectrum of our samples containing LHC II, extracted from spinach leaves, was recorded using a simple Ocean Optics lamp and spectrometer (USB2000) at room temperature, and is shown in Fig. 11. This spectrum shows similar shapes and peak positions to those reported in the literature.[43] The absorption spectrum shows one main peak in the red region at about 675 nm, which is due mainly to chlorophyll *a*,[44] and a shoulder at 650 nm, which is related mostly to chlorophyll *b*. In addition, the absorption spectrum exhibits a broadband from 400 nm to 520 nm, with the main peak positioned at 440 nm and shoulders on both sides. The peak at 440 nm represents chlorophyll *a*, while the peak at 467 nm represents chlorophyll *b*—both in the blue absorption region of LHC II.[29]

The preparation of the LHC II from PS II also indicated the presence of CP47 and CP43, which are complexes from the peripheral core complex of PS II, and D1 and D2 proteins closely

associated to the reaction centre, as shown in Fig. 3. We also noticed the presence of LHC I residual in the sample, as indicated in Fig. 3. By using a set of adjustable filters, the pump pulse energy was set to 2 μJ and the beam size at the focus was about 300 μm. The sample was inserted into a rotating glass cell to ensure fresh sample for every pulse, in order to avoid sample degradation and to prevent the accumulation of long-lived states. Figure 12 shows the transient absorption spectra obtained in the region from 350 nm to 800 nm, although the white light continuum only had significant intensity from 420 nm to 700 nm. In this case, in order to excite both chlorophyll *a* and chlororphyll *b* components, the LHC II sample was pumped by a wavelength of 610 nm. Although 610 nm does not correspond to the peak absorption wavelength, our system provided high pulse energies and good pulse to pulse stability at this wavelength. Figure 12 shows five broadband absorbance changes of interest. The negative absorbance changes with peaks at 436 nm and 678 nm correspond to ground-state bleaching of chlorophyll *a*. The pump excites many molecules into the higher excited state, which results in a reduction of the number of molecules in the ground state. Therefore, when the probe pulse arrives, there are fewer molecules in the ground state, causing negative absorbance changes. The broadband positive absorbance change (about 500–640 nm), with a peak at about 542 nm, is due to excited state absorption. This signal is caused by the excited state population, which is then excited further to a higher energy level by the probe pulse. This causes an increase of the absorption of the probe beam. In addition, shoulder bands observed at 472 nm (Fig. 12, outer graph) and 650 nm (Fig. 12, inner graph) can be ascribed to ground-state bleaching of chlorophyll *b*. However, the large contribution of the broadband excited state absorption (positive absorbance change from 500 nm to 640 nm) resulted in a less pronounced chlorophyll *b* shoulder at 650 nm than expected. The peak observed at 610 nm is as a result of laser scatter from the sample, due to particles in the sample, indicating imperfect sample preparation. At 610 nm, chlorophyll *a* and *b* are excited and energy transfers are expected to occur between the chlorophyll molecules. Several studies on the energy transfer between the chlorophylls have shown that the transfer usually takes place from chlorophyll *b* to chlorophyll *a*.[3,45] In addition to the transfer from chlorophyll *b* to chlorophyll *a*, there is also energy equilibration that takes place from chlorophyll *a* to chlorophyll *a* and from chlorophyll *b* to chlorophyll *b*. The LHC II monomer is composed of 7–8 chlorophyll *a* molecules, 4–5 chlorophyll *b* molecules and 3 carotenoids, at a chlorophyll *a*:*b* ratio of 1.6:2. The energy transfer from chlorophyll *b* to chlorophyll *a*, within this monomer, exhibits three components: a very fast component that occurs at about 100–150 fs and two other components that have lifetimes of 600–800 fs and 5–7 ps.[45]

In order to obtain complete information on the five bands observed in Fig. 12, a contour graph can be plotted (Fig. 13). Figure 13 shows the transient absorption of LHC II as a function of wavelength and relative delay time between pump and probe. It is possible to observe the pump at 610 nm in this case, which remains constant over all experimental time delays and is due to laser scatter. In addition, the variation of the ground-state bleaching at 678 nm and 436 nm, and the excited state absorption with a peak at about 542 nm, can be clearly observed.

To extract further information regarding the time constants of the energy transfer of the LHC II from the experiment, the spectra are actually measured at a large number of delay times, such that specific fast absorption changes can be temporally quantified and their time constants extracted. Figure 14 shows the evolution of the absorbance changes of 678 nm (the strongest absorption in Fig. 11), 542 nm, 472 nm and 436 nm as a function of delay time. In the 678-nm, 472-nm and 436-nm bands, we observed a fast drop in the absorbance change to quickly reach a minimum, followed by a slow recovery. In the 542-nm transient we observed a fast increase followed by a slow downturn. To obtain the time constants, we applied a second-order exponential fit procedure to the data set obtained at each peak (436 nm, 472 nm, 548 nm and 678 nm). This was done because we

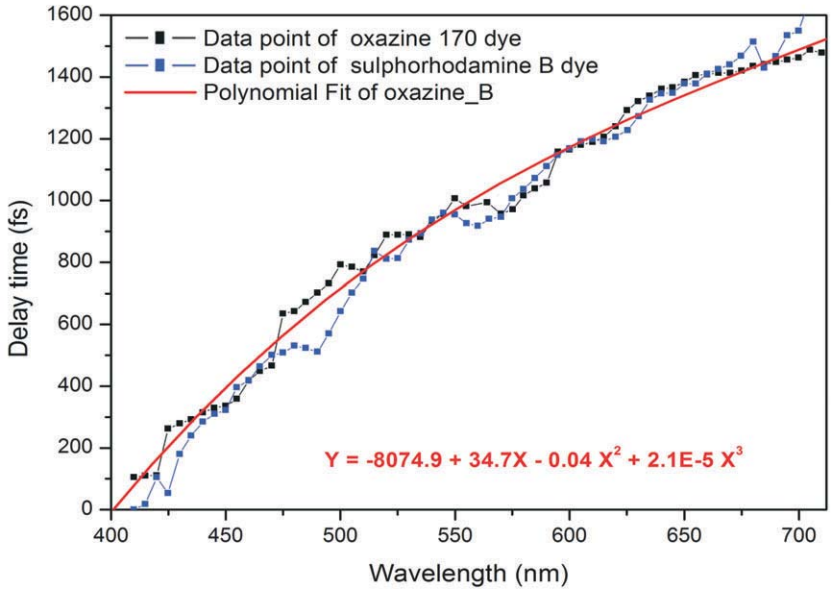

Fig. 10. Plot of relative time delay against wavelengths of Oxazine 170 and sulphorhodamine dyes, with polynomial fit to Oxazine 170 data and the time correction equation for chirp.

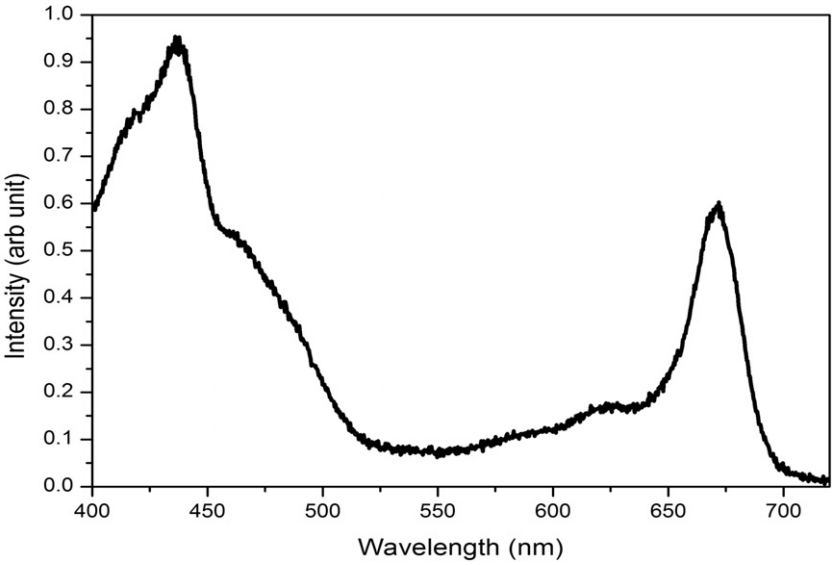

Fig. 11. Absorption spectrum of LHC II extracted from spinach leaves (recorded at room temperature).

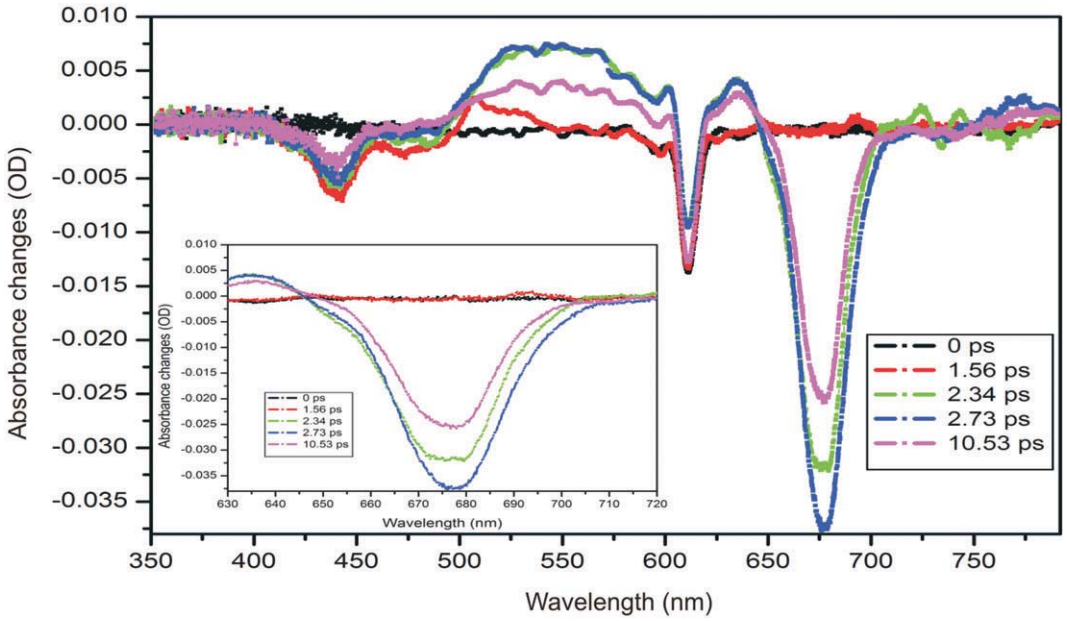

Fig. 12. Transient absorption of LHC II in the indicated wavelength interval and time delays with the pump wavelength set at 610 nm (outer graph) and the transient absorption of LHC II in the 630–720 nm region which clearly indicates the shoulder at 650 nm (inner graph).

expected the sample to exhibit at least two separate energy transfer mechanisms with different time constants, and because a single exponential did not fit the data well. The experimental values of the energy transfer time constants are tabulated in Table 1. The results of the second-order exponential fit gave us two time constants, 1.3 ± 0.5 ps and 25 ± 4 ps, for the 678-nm peak. The 1.3-ps time constant can be ascribed to singlet-singlet annihilation within the LHC II monomer and the 24.5-ps component to the annihilation in the trimer. Comparable time constants, 1.9 ps and 20 ps, for monomer and trimer annihilation, respectively, at 679 nm have been reported.[46] This process could limit the energy transfer.[46]

In the blue absorption region, we were able to detect the time constants of energy transfer between chlorophylls. The 436-nm peak relates to chlorophyll *a* and gives us two time constants (860 ± 200 fs and 45 ± 4 ps), whereas the 472-nm peak relates to chlorophyll *b* and gives two time constants (750 ± 100 fs and 29 ± 2 ps). The 29-ps and 45-ps time constants are not accurate extracted values since the measurement was done only over a total range of 15 ps. However, the time constant of 750 fs is related to the energy transfer from chlorophyll *b* to chlorophyll *a* and is reflected in the disappearance of the chlorophyll *b* bleaching (472-nm peak) after about 800 fs, as indicated in Fig. 12. The time constant of the major component of energy transfer from chlorophyll *b* to chlorophyll *a* was reported in the literature to be about 600 fs.[3,45–48]

Time constants obtained for 542 nm are 4.76 ± 1 ps and 43 ± 6 ps, again the latter value is less accurate due to the limited range of the experimental measurement. This broadband feature, from 500 nm to 600 nm (with peak at 542 nm), is related to the relaxation of the vibrational energy of the excited state of the chlorophyll molecules. Upon excitation at 610 nm, the

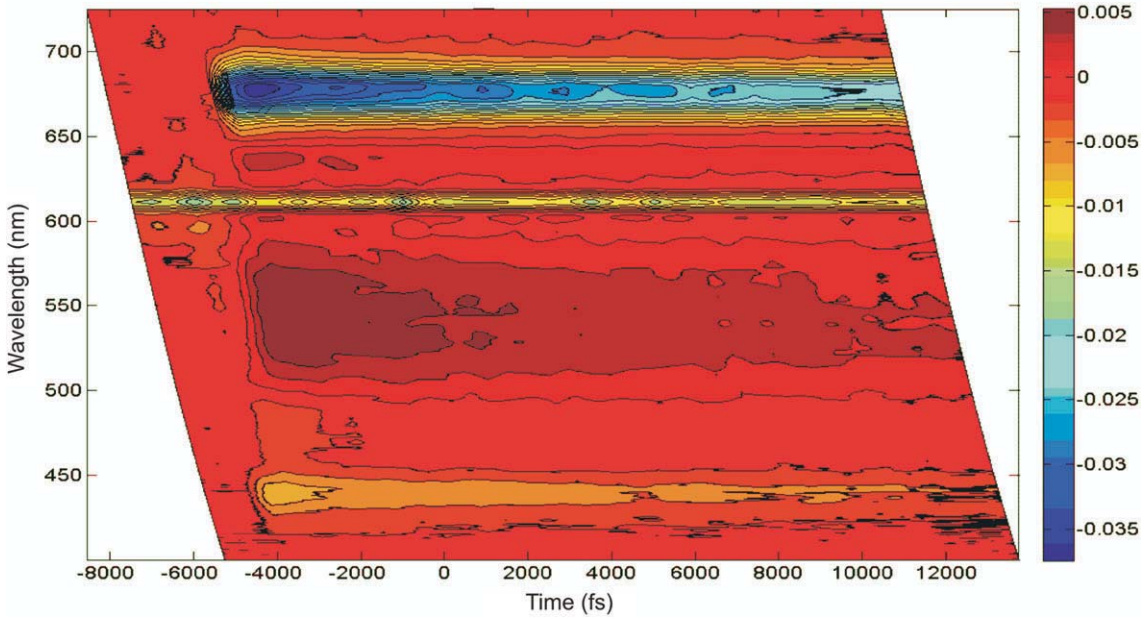

Fig. 13. Transient absorption contour graph indicating measured absorbance changes in OD for a range of delay times between pump and probe pulses. Pump was set at 610 nm and probe was a white light continuum. The chirp correction equation was applied to the data.

molecules are excited to a high vibrational energy level of the electronic excited state. The molecules will then undergo vibrational relaxation. Therefore the probe gives us a broadband spectrum which is the overlap of absorption spectra of molecules in different vibrational energy levels.

The time constants obtained for LHC II for the absorbance changes at 678 nm correspond well with those expected, while the others are less accurate, probably due to a long-lived state being populated and not resolved temporally here due to its long lifetime. The observation of a long-lived state could be due to the presence of LHC I, D1 and D2 residue in our sample. These complexes are expected to have long lifetimes, in the order of hundreds of picoseconds up to the nanosecond regime.

The transient absorption experiment was also carried out at different pump wavelengths in order to compare results obtained for the energy transfer times from different degrees of pump excitation. Figure 15 indicates the absorbance changes of the same sample, containing LHC II, pumped at different wavelengths: 610 nm, 630 nm, 650 nm and 680 nm at zero time delay (or strongest absorption change). As expected, we observed the strongest absorbance changes, about 0.052 OD, when the pump was set at 680 nm. The pump of 650 nm, 630 nm and 610 nm produced the strongest absorption changes of 0.027 OD, 0.020 OD and 0.013 OD, respectively. By changing the pump wavelengths, we excited different pigments (chlorophyll *a*, chlorophyll *b* or chlorophyll *a*/*b*), which resulted in different energy transfer processes taking place; in other words, different combinations of chlorophyll *b* to chlorophyll *a* energy transfers and chlorophyll *a* to chlorophyll *a* energy transfers occurred. Different time constants are therefore expected.

Time constants extracted from each of these experiments for the 678-nm peak are given in Table 2. By setting the pump at 650 nm, which is the strongest chlorophyll *b* absorption wavelength, we were able to observe two time constants, 0.81 ± 0.3 ps and 9.95 ± 1 ps, related to the energy transfer from chlorophyll *b* to chlorophyll *a*. These values compare well with the values of 600 fs and 5–7 ps reported in the literature.[3,45,47,48] The excitation of the sample at 680 nm gave us time constants of about 0.35 ± 0.1 ps and 6.90 ± 0.3 ps. These values are correlated to the chlorophyll *a* to chlorophyll *a* energy equilibration and are in agreement with the values reported in the literature,[48] which are 300 fs and 6 ps. By changing the pump wavelength to 630 nm, we obtained 2.8 ± 1.1 ps and 47 ± 17 ps; these long times could be due to internal conversion.

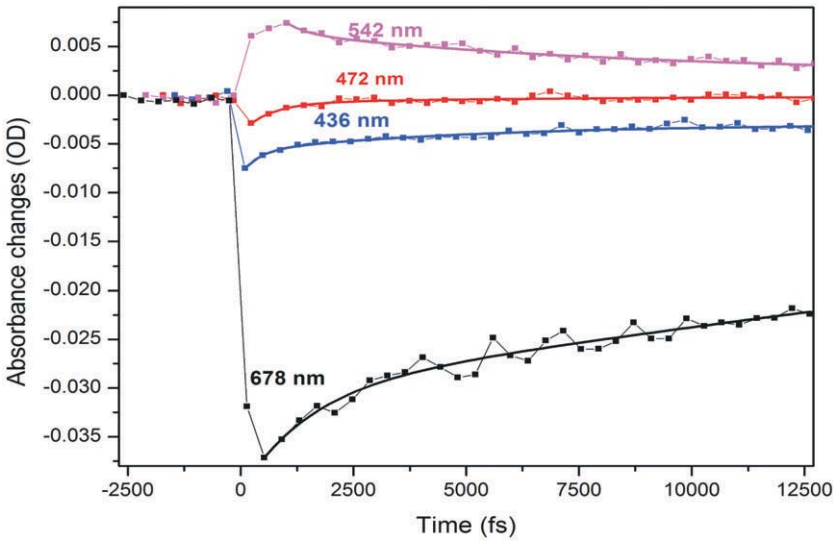

Fig. 14. Absorbance change as a function of relative delay time between pump and probe pulses for LHC II at different wavelengths (436 nm, 472 nm, 542 nm and 678 nm) pumped at 610 nm, after the chirp correction equation was applied.

Table 1. Summary of observed time constants at different probe wavelengths (436 nm, 472 nm, 542 nm and 678 nm) for a pump wavelength of 610 nm.

Probe wavelength	436 nm	472 nm	542 nm	678 nm
t_1(ps)	0.86 ± 0.2	0.75 ± 0.1	4.76 ± 1	1.3 ± 0.5
t_2(ps)	45 ± 4	29 ± 2	43 ± 6	25 ± 4

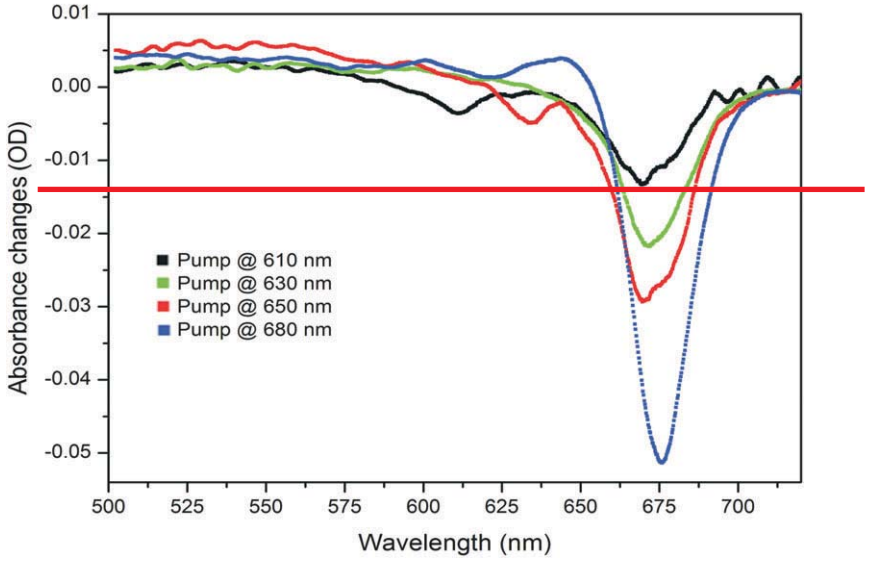

Fig. 15. Transient absorption of LHC II of sample from spinach leaves for different pump wavelengths. The spectra was recorded at relative time t = 0 when the pump and probe overlap.

Table 2. Summary of observed time constants at different pump wavelengths (610 nm, 630 nm, 650 nm and 680 nm) for a probe wavelength of 678 nm.

Pump wavelength	610 nm	630 nm	650 nm	680 nm
t_1(ps)	1.3 ± 0.5	2.8 ± 1.1	0.81 ± 0.3	0.35 ± 0.1
t_2(ps)	25 ± 4	47 ± 17	9.95 ± 1	6.90 ± 0.3

In the present study, the ultrafast energy transfer components which occurred in less than 200 fs were not resolved due to the temporal limitation of our setup. Some values did not correspond well with those reported in the literature—an indication that a longer time range measurement is required for more accurate exponential fit procedures. The process may also be more complicated than consisting of only two time constants. These are challenges for future work in improvements in the extracted time constants and interpretation thereof.

Conclusions and future work

We have presented the development of a technique of femtosecond pump probe spectroscopy for ultrafast time-resolved spectroscopy, and the preliminary results achieved using this technique. Our experimental setup was standardised using Malachite green dye and the measured lifetime of 2.9 ps corresponds well to those reported in the literature for this dye. We presented our method of correcting for the chirp induced in the white light continuum generation process, as this is required for accurate time resolution of the measurements. We have also presented preliminary measurements of the ultrafast energy transfer in light-harvesting complexes extracted from spinach leaves. Upon excitation at 610 nm, we were able to measure the time constants of the energy transfer between the chlorophylls, as well as annihilation processes. Future work involves the detailed study of the energy transfer lifetimes as a function of pump laser intensity and wavelength, optimisation and confirmation of the ultrafast dynamics of the extracted light-harvesting complexes, as well as further work in interpretation of energy transfer information from the pump probe measurements.

The ultimate goal is to use this technique to characterise the light-harvesting and energy-transfer characteristics of artificial systems developed at the CSIR, and to compare these with natural systems. The work proposed by this group focuses on the development of artificial light-harvesting and energy-transfer systems which match the rates and efficiencies of the natural photosynthetic systems. Two approaches are being pursued. One approach uses porphyrins and produces nanorod structures via ionic self-assembly. These porphyrin nanorods are then embedded in a polymeric scaffold to enhance the structural properties of the nanorods. The second approach uses a polymeric scaffold and attach porphyrins to specific sites on the polymer backbone. The polymer acts to produce specific architectures for site-directed energy transfer. The aim will be to produce structures for which the direction of energy transfer is defined. The next step is to produce technical specifications for the energy-transfer system in terms of the direction, rate and efficiency of the energy-transfer process and robustness of the system.

Received 10 March. Accepted 3 September 2009.

1. Zinth W. and Wachtveitl J. (2005). The first picoseconds in bacterial photosynthesis – ultrafast electron transfer for the efficient conversion of light energy. *Chem. Phys. Chem.* **6**, 871–880.
2. Cogdell R.J., Issacs N.W., Howard T.D., McLuskey K., Fraser N.J. and Prince S.M. (1999). How photosynthetic bacteria harvest solar energy. *J. Bacteriol.* **181**, 3869–3879.
3. Van Grondelle R. and Novoderezhkin V.I .(2006). Energy transfer in photosynthesis: experimental insights and quantitative models. *Phys. Chem. Chem. Phys.* **8**, 793–807.
4. Mančal T., Valkunas L., Read E.L., Engel G.S., Calhoun T.R. and Fleming G.R. (2008). Electronic coherence transfer in photosynthetic complexes and its signatures in optical spectroscopy. *Spectroscopy* **22**, 199–211.
5. Liu Z., Yan H., Wang K., Kuang T., Zhang J., Gul L., An X. and Chang W. (2004). Crystal structure of spinach major light-harvesting complex at 2.72 Å resolution. *Nature* **428**, 287–292.
6. McDermott G., Prince S.M., Freer A.A., Hawthornthwaite-Lawless A.M., Papiz M.Z., Cogdell R.J. and Isaacs N.W. (1995). Crystal structure of an integral membrane light-harvesting complex from photosynthetic bacteria. *Nature* **374**, 517–521.
7. Müh F., Renger T. and Zouni A. (2008). Crystal structure of cyanobacterial photosystem II at 3.0 Å resolution: a closer look at the antenna system and the small membrane-intrinsic subunits. *Plant Physiol. Biochem.* **46**, 238–264.
8. Conçalves R.P., Busselez J., Lévy D., Seguin J. and Scheuring S. (2005). Membrane insertion of *Rhodopseudomonas acidophila* light-harvesting complex 2 investigated by high resolution AFM. *J. Struct. Biol.* **149**, 79–86.
9. Bahatyrova S., Frese R.N., Siebert C.A., Olsen J.D., van der Werf K.O., van Grondelle R., Niederman R.A., Bullough P.A., Otto C. and Hunter C.N. (2004). The native architecture of a photosynthetic membrane. *Nature* **430**, 1058–1062.
10. Scheuring S., Boudier T. and Sturgis J.N. (2007). From high-resolution AFM topographs to atomic models of supramolecular assemblies. *J. Struct. Biol.* **159**, 268–276.
11. Goc J., Hara M., Tateishi T. and Miyake J. (1996). Reconstructed light-harvesting system for photosynthetic reaction centres. *J. Photochem. Photobiol. A: Chem.* **93**, 137–144.
12. Kramer H., Jones M.R., Fowler G.J.S., Francke C., Aartsma T.J., Hunter C.N. and Amez J. (1995). Energy migration in *Rhodobacter spaeroides* mutants altered by mutagenesis of the peripheral LH2 complex or by removal of the core LHI complex. *Biochim. Biophys. Acta.* **1231**, 89–97.
13. Zuber H. and Cogdell R. (1995). Structure and organisation of purple bacterial antenna complexes. In *Anoxygenic Photosynthetic Bacteria,* eds R. Blankenship, M. Madigan and C. Bauer, pp. 315–348. Kluwer Academic Publishers, Dordrecht, the Netherlands.
14. Zuber H. and Brunisholz R.A. (1991). Structure and function of antenna polypeptides and chlorophyll protein complexes: principles and versatility. In *The Chlorophylls,* ed. H. Scheer, pp. 627–703. CRC Press, Boca Raton, Florida.
15. Hu X., Damjanovic A., Ritz T. and Schulten K. (1998). Architecture and mechanism of the light-harvesting apparatus of purple bacteria. *Proc. Natl. Acad. Sci. USA* **95**, 5935–5941.
16. Harvey P.D., Stern C., Gros C.P. and Guilard R. (2008). Comments on the through-space singlet energy transfers and energy migration (exciton) in the light-harvesting systems. *J. Inorg. Biochem.* **102**, 395–405.
17. Visser H.M., Somsen O.J.G., van Mourik F., Lin S., van Stokkum I.H.M. and van Grondelle R. (1995). Direct observation of sub-picosecond equilibration of excitation energy in the light-harvesting antenna of *Rhodospirillum rubrum. Biophys. J.* **89**, 1083–1099.
18. Bradforth S.E., Jimenez R., van Mourik F., van Grondelle R. and Fleming G.R. (1995). Excitation transfer in the core light-harvesting complex (LH-1) of *Rhodobacter sphaeroides:* an ultrafast fluorescence depolarization and annihilation study. *J. Phys. Chem.* **99**, 16179–16191.
19. Hess S., Chachisvilis M., Timpmann K., Jones M.R., Fowler G.J.S., Hunter C.N. and Sundström V. (1995). Temporally and spectrally resolved sub picosecond energy transfer within the peripheral antenna complex (LH2) and from LH2 to the core antenna complex in photosynthetic purple bacteria. *Proc. Natl. Acad. Sci. USA* **92**, 12333–12337.
20. Visscher K.J., Bergström H., Sundström V., Hunter C.N. and van Grondelle R. (1989). Temperature dependence of energy transfer from the long wavelength antenna BChl-896 to reaction center in *Rhodospirillum rubrum, Rhodobacter sphaeroides* (w.t. and M21 mutant) from 77 to 177 k, studied by picosecond absorption spectroscopy. *Photosynth. Res.* **22**, 211–217.
21. Gradinaru C.C., Kennis J.T.M., Papagiannakis E., van Stokkum I.H.M., Cogdell R.J., Fleming G.R., Niederman R.A. and van Grondelle R. (2001). An unusual pathway of excitation energy deactivation in carotenoids: singlet-to-triplet conversion of an ultrafast timescale in a photosynthetic antenna. *Proc. Natl. Acad. Sci. USA* **98**, 2364–2369.
22. Groot M.L., Breton J., van Wilderen L.J.G.W., Dekker J.P. and van Grondelle R. (2004). Femtosecond visible/visible and visible/mid-IR pump-probe study of the photosystem II core antenna complex CP47. *J. Phys. Chem. B* **108**, 8001–8006.
23. Doust A.B., van Stokkum I.H.M., Larsen D.S., Wilk K.E., Curmi P.M.G., van Grondelle R. and Scholes G.D. (2005). Mediation of ultrafast light-harvesting by a central dimer in phycoerythrin 545 studied by transient absorption and global analysis. *J. Phys. Chem. B* **109**, 14219–14226.
24. Croce R., Cinque G., Holzwarth A.R. and Bassi R. (2000). The soret absorption properties of carotenoids and chlorophylls in antenna complexes of higher plants. *Photosynth. Res.* **64**, 221–231.
25. Jansson S. (1994). The light-harvesting chlorophyll a/b-binding proteins. *Biochim. Biophys. Acta* **1184**, 1–19.
26. Van Oort B., van Hoek A., Ruban A.V. and van Amerongen H. (2007). Aggregation of light-harvesting complex II leads to formation of efficient excitation energy traps in monomeric and trimeric complexes. *Fed. Eur. Biochem. Soc. Lett.* **581**, 3528–3532.
27. Nield J. and Barber J. (2006). Refinement of the structural model for the photosystem II supercomplex of higher plants. *Biochim. Biophys. Acta* **1757**, 353–361.
28. De Weerd F.L., van Stokkum I.H.M., van Amerongen H., Dekker J.P. and van Grondelle R. (2002). Pathways for energy transfer in the core light-harvesting complexes CP43 and CP47 of photosystem II. *Biophys. J.* **82**, 1586–1597.
29. Kühlbrandt W., Wang D.N. and Fujiyoshi Y. (1994). Atomic model of plant light-harvesting complex by electron crystallography. *Nature* **367**, 614–621.
30. Gradinaru C.C., van Stokkum I.H.M., Pascal A.A., van Grondelle R. and van Amerongen H. (2000). Identifying the pathways of energy transfer between carotenoids and chlorophylls in LHC II and CP 29. A multicolor, femtosecond pump-probe study. *J. Phys. Chem. B* **104**, 9330–9342.
31. Novoderezhkin V.I., Palacios M.A., van Amerongen H. and van Grondelle R. (2005). Excitation dynamics in the LHC II complex of higher plants: modeling based on the 2.72 Å crystal structure. *J. Phys. Chem. B* **109**, 10493–10504.
32. Simidjiev I., Barzda V., Mustárdy L. and Garab G. (1997). Isolation of lamellar aggregates of the light-harvesting chlorophyll a/b protein complex of photosystem II with long-range chiral order and structural flexibility. *Anal. Biochem.* **250**, 169–175.
33. Lambrev P.H., Várkonyi Z., Krumova S., Kovács L., Miloslavina Y., Holzwarth A.R. and Garab G. (2007). Importance of trimer–trimer interactions for the

native state of the plant light-harvesting complex II. *Biochim. Biophys. Acta.* **1767**, 847–853.

34. Cerullo G., Manzoni C., Luer L. and Polli D. (2007). Time-resolved methods in biophysics 4. Broadband pump-probe spectroscopy system with sub-20 fs temporal resolution for the study of energy transfer processes in photosynthesis. *Photochem. Photobiol. Sci.* **6**, 135–144.
35. Chen H.Y., Lee I.R. and Cheng P.Y. (2006). Gas-phase femtosecond transient absorption spectroscopy. *Rev. Sci. Instrum.* **77**, 076105.
36. Reid G.D. and Wynne K. (2000). Ultrafast laser technology and spectroscopy. In *Encyclopedia of Analytical Chemistry,* ed. R.A. Meyers, pp. 13644–13670. John Wiley & Sons, Chichester.
37. Fukuda M., Kajimoto O., Terazima M. and Kimura Y. (2007). Application of the transient grating method to the investigation of the photo-thermalization process of Malachite green in room temperature ionic liquids. *J. Mol. Liquids* **134**, 49–54.
38. Schweitzer G., Xu L., Craig B. and DeSchryver F.C. (1997). A double OPA femtosecond laser system for transient absorption spectroscopy. *Optics Comm.* **142**, 283–288.
39. Palacios R.E., Kodis G., Gould S.L., de la Garza L., Brune A., Gust D., Moore T.A. and Moore A.L. (2005). Artificial photosynthetic reaction centers: mimicking sequential electron and triplet energy transfer. *Chem. Phys. Chem* **6**, 2359–2370.
40. Wasielewski M.R. (2006). Energy, charge and spin transport in molecules and self-assembled nanostructures inspired by photosynthesis. *J. Organ. Chem.* **71**, 5051–5066.
41. Hori T., Aratani N., Takagi A., Matsumoto T., Kawai T., Yoon M.C., Yoon Z.S., Cho S., Kim D. and Osuka A. (2006). Giant porphyrin wheels with large electronic coupling as models of light-harvesting photosynthetic antenna. *Chem – A Eur. J.* **12**, 1319–1327.
42. Katterle M., Prokhorenko V.I., Holzwarth A.R. and Jesorka A. (2007). An artificial supramolecular photosynthetic unit. *Chem. Phys. Lett.* **447**, 284–288.
43. Krupa Z., Huner N.P.A., Williams J.P., Maissan E. and James D.R. (1987). Development at cold hardening temperatures – the structure and composition of purified rye LHCII. *Plant Physiol.* **84**, 19–24.
44. Holt N.E., Kennis J.T.M. and Fleming G.R. (2004). Femtosecond fluorescence upconversion studies of light-harvesting β-carotene in oxygenic photosynthetic core proteins. *J. Phys. Chem. B* **108**, 19029–19035.
45. Palacios M.A., Standfuss J., Vengris M., van Oort B.F., van Stokkum I.H.M., Kuhlbrandt W., van Amerongen H. and van Grondelle R. (2006). Comparison of the three isoforms of the light-harvesting complex II using transient absorption and time resolved fluorescence measurement. *Photosynth. Res.* **88**, 269–285.
46. Visser H.M., Kleima F.J., van Stokkum I.H.M., van Grondelle R. and van Amerongen H. (1996). Probing the many energy-transfer processes in the photosynthetic light-harvesting complex II at 77 K using energy-selective sub-picosecond transient absorption spectroscopy. *Chem. Phys.* **210**, 297–312.
47. Croce R., Müller M.G., Bassi R. and Holzwarth A.R. (2003). Chlorophyll b to chlorophyll a energy transfer kinetics in the CP29 antenna complex: a comparative femtosecond absorption study between native and reconstituted proteins. *Biophys. J.* **84**, 2508–2516.
48. Croce R., Müller M.G., Bassi R. and Holzwarth A.R. (2001). Carotenoid-to-chlorophyll energy transfer in recombinant major light-harvesting complex (LHCII) of higher plants. I: Femtosecond transient absorption measurements. *Biophys. J.* **80**, 901–915.